

1 **Conserved association of Argonaute 1 and 2 proteins with miRNA and siRNA**
2 **pathways throughout insect evolution, from cockroaches to flies**

3

4

5 Mercedes Rubio, Jose Luis Maestro, Maria-Dolors Piulachs and Xavier Belles*

6 Institute of Evolutionary Biology (CSIC-UPF), Passeig Marítim 37, 08003 Barcelona

7

8

9 *Corresponding author, e-mail: xavier.belles@ibe.upf-csic.es

10

12 ABSTRACT

13

14 *Background:* Argonaute proteins are key in RNA silencing. In *Drosophila*
15 *melanogaster*, the five proteins of the Argonaute family participate in the pathways and
16 mechanisms mediated by three types of small RNAs: piRNAs, miRNAs, and siRNAs.
17 Two Argonaute proteins, Argonaute 1 (Ago1) and Argonaute 2 (Ago2), are associated
18 with miRNA and siRNA mechanisms, which are the most thoroughly studied. The
19 available data points to a sorting specialization of Ago1 for miRNAs and Ago2 for
20 siRNAs. However, this has been demonstrated only in *D. melanogaster*, one of the most
21 modified insects, which emerged some 100 million years ago. Thus, an important
22 question is whether this association of Ago1 with miRNAs and Ago2 with siRNAs
23 occurs generally in insects, or was a specific innovation in higher flies.

24 *Methods:* We addressed this question by using RNAi approaches and studying Ago1
25 and Ago2 functions in the German cockroach, *Blattella germanica*, a much less
26 modified insect that emerged some 320 million years ago.

27 *Results:* The results showed that *B. germanica* does preferentially use Ago1 in the
28 miRNA pathway, but can also use Ago2 in some cases. Conversely, Ago2 operates in
29 the RNAi, in siRNA sorting, whereas Ago1 seems to have no relevant role in this
30 process.

31 *Conclusions and general significance:* These basic associations are equivalent to those
32 observed in *D. melanogaster*, implying that they have been evolutionary conserved
33 from at least cockroach to flies, and possibly stem from the last common ancestor of
34 extant insects.

35

36

37

38

39 *Keywords:* Argonaute proteins; RNAi; miRNA; siRNA; *Blattella*; *Drosophila*.

40

41

42

43

45 **1. Introduction**

46

47 RNA interference (RNAi) pathways mediated by small RNAs have been
48 reported throughout eukaryotic organisms, suggesting that they were present in the last
49 common ancestor of all extant eukaryotes. RNAi mechanisms possibly originated to
50 counteract viral invasion, and were later coopted for other functions, like post-
51 transcriptional regulation of gene expression (Shabalina and Koonin, 2008). Although
52 the basic structure of RNAi pathways is similar in all eukaryotes studied, gene
53 duplication and gene loss has occurred in multiple lineages, and work on model
54 organisms has shown that the duplication and loss of core RNAi pathway genes has
55 occurred multiple times (Dowling et al., 2016). A notable example is provided by the
56 Argonaute proteins, which are at the core of all RNAi pathways (Kuhn and Joshua-Tor,
57 2013; Meister, 2013) and notably vary in number in different groups, from 26 in the
58 nematode *Caenorhabditis elegans* to 5 in the fly *Drosophila melanogaster* (Lewis et al.,
59 2016; Swarts et al., 2014).

60 In *D. melanogaster*, the five proteins in the Argonaute family participate in the
61 three pathways and mechanisms respectively mediated by three types of small RNAs:
62 Piwi interacting RNAs (piRNAs), microRNAs (miRNAs), and small interfering RNAs
63 (siRNAs). Three *D. melanogaster* Argonaute proteins that belong to the Piwi subfamily
64 (Piwi, Argonaute 3 and aubergine) are associated with piRNA mechanisms (Hartig et
65 al., 2007; Siomi et al., 2011). The main function of piRNAs is to counteract the action
66 of mobile elements in the genome through binding to Piwi subfamily proteins (Siomi et
67 al., 2011). The other two Argonaute proteins of *D. melanogaster*, Argonaute 1 (Ago1)
68 and Argonaute 2 (Ago2), are associated with miRNA and siRNA mechanisms, which
69 are the most thoroughly studied (Carthew and Sontheimer, 2009).

70 miRNAs are processed from the corresponding hairpin miRNA precursor by an
71 endonuclease called Dicer, which was discovered by Hannon's group (Bernstein et al.,
72 2001) in *D. melanogaster*. Processing yields two partially complementary single strand
73 miRNAs: the "mature" miRNA and the "passenger" strand. In insects, this duplex is
74 incorporated into the RNA-induced silencing complex (RISC) combined with the
75 protein Argonaute, discovered by Tuschl's group (Martinez et al., 2002), where the
76 "mature" miRNA is selected. The miRNA then guides the Ago-RISC to the target
77 mRNA, the miRNA binds to its target site in the mRNA by imperfect complementarity,
78 and blocks transcript translation (Bartel, 2009)(see also (Belles et al., 2012) for a

79 comprehensive history of the discovery of the mechanisms regulating miRNA
80 production and action). siRNAs are generated from long double-stranded RNAs
81 (dsRNAs) that can be endogenous or exogenous in origin. The dsRNA is cleaved into
82 siRNAs by a Dicer enzyme, then the siRNAs unwind, the guide strand couples to an
83 Ago-containing RISC, which conveys it to the target mRNA. Finally the RISC couples
84 to the target mRNA, blocking and degrading it (Siomi and Siomi, 2009) (see also
85 (Belles, 2010) for a comprehensive history of the discovery of the mechanisms
86 regulating RNAi).

87 The above data point to a sorting specialization of different Dicer enzymes and
88 Ago proteins for miRNAs and siRNAs in insects. In mammals, a single Dicer assort
89 siRNAs and miRNAs among four Ago proteins, apparently without much
90 discrimination (Czech and Hannon, 2011). In *D. melanogaster* there are two Dicer
91 enzymes, Dicer-1 and Dicer-2, which, in general, are involved in the miRNA and
92 siRNA pathways, respectively (Lee et al., 2004), whereas a parallel sorting
93 specialization of Ago1 for miRNAs and Ago2 for siRNAs has been reported in the same
94 fly (Czech and Hannon, 2011; Czech et al., 2009). This specialization would look as a
95 general rule for insects, but in fact it has been demonstrated only in *D. melanogaster*,
96 one of the most derived and modified insects on Earth, making it rather unrepresentative
97 of the insect class. Indeed, drosophilids are relative newcomers in the evolutionary
98 history of insects, as they emerged in mid-Cretaceous, some 100 million years ago
99 (Grimaldi and Engel, 2005). An important question is, therefore, whether this parallel
100 association of Ago1 with miRNAs and Ago2 with siRNAs is general in insects, or was a
101 specific innovation of higher flies.

102 We have addressed this question by using in the German cockroach *Blattella*
103 *germanica* as experimental subject. Cockroaches are an ancient group that emerged in
104 the mid-Carboniferous, some 320 million years ago. They show many features that can
105 be presumed to be similar to those of the last common ancestor of winged insects, such
106 as short germ-band embryogenesis and hemimetabolan metamorphosis. This contrasts
107 with *D. melanogaster*, a long germ-band, holometabolan species (Ylla et al., 2017).
108 Moreover, *B. germanica* is highly sensitive to RNAi (Belles, 2010), making it
109 particularly suitable for experimental gene silencing using this approach. In previous
110 papers, we studied the role of Dicer-1 in the miRNA pathway (Gomez-Orte and Belles,
111 2009) and Dicer-2 in the siRNA pathway (Lozano et al., 2012). In the present work we

112 wondered whether Ago1 and Ago2 are also respectively specialized in miRNA and
113 siRNA pathways in *B. germanica*.

114

115 **2. Materials and methods**

116

117 *2.1. Insect sampling and RNA extraction*

118

119 Freshly ecdysed fifth (penultimate) instar nymphs (N5) of the cockroach *B.*
120 *germanica* used in the experiments were obtained from a colony reared in the dark at 30
121 \pm 1°C and 60-70% relative humidity. The entire animal except the head (to avoid
122 interferences with the eye pigments) and the digestive tube (to avoid contamination with
123 parasites) was used for RNA extractions. All dissections and tissue sampling were
124 carried out on carbon dioxide-anaesthetized insects. RNA isolation was carried out with
125 miRNeasy® Mini Kit (QUIAGEN), which increases the yield of small RNAs. The
126 reverse transcription was carried out with the NCode™ miRNA First-Strand cDNA
127 Synthesis and qRT-PCR Kits (Invitrogen), following the manufacturer's protocols,
128 which allows the quantification of the mRNA and miRNAs by quantitative real-time
129 PCR (qRT-PCR). Only in the experiment examining the effect of a dsRNA on Ago2
130 expression, RNA was extracted with the GenElute Mammalian Total RNA kit (Sigma),
131 and cDNA was prepared with the Transcriptor First Strand cDNA Synthesis kit
132 (Roche).

133

134 *2.2. Phylogenetic analysis*

135

136 We obtained the insect sequences labeled as Ago1 and Ago2 from GenBank, and
137 from i5k project (<https://i5k.nal.usda.gov/webapp/blast/>) (Poelchau et al., 2015) by
138 BLAST search using the protein sequences from *B. germanica* and *D. melanogaster* as
139 queries. Finally, the species and protein sequences of Ago1 and Ago2 included in the
140 analysis were those indicated in Supplementary Table S1. As external group, we used
141 the Ago3, Piwi and aubergine sequences of *D. melanogaster* and *B. germanica*
142 (Supplementary Table S1). Alignments were carried out with ClustalX (Larkin et al.,
143 2007) and phylogenetic reconstruction with RAxML (Stamatakis, 2014), based on the
144 maximum-likelihood principle, a JTT matrix, a gamma model of heterogeneity rate, and

145 using empirical base frequencies and estimating proportions. The data was bootstrapped
146 for 100 replicates.

147

148 *2.3. Characterization of the miRNAs studied*

149 We examined the expression of the following mature miRNAs: bantam (bantam-
150 3-p), let-7 (let-7-5p), miR-1 (miR-1-3p), miR-10 (miR-10-5p), miR-34 (miR-34-5p),
151 miR-184 (miR-184-3p) and miR-276 (miR-276-3p). In the case of miR-10 and miR-
152 276, we also examined the “passenger” strand: miR-10* (miR-10-3p) and miR-276*
153 (miR-276-5p). The discrimination between the mature and passenger strand is based on
154 the level of expression (higher in the mature than in the passenger), as detailed in the
155 Supplementary Data S1 of Ylla et al. (2016).

156

157 *2.4. Quantification by qRT-PCR*

158

159 For mRNA expression studies by qRT-PCR, 400 ng of total RNA were reverse
160 transcribed. Amplification reactions were carried out using iQ™ SYBR Green
161 Supermix (BioRad) and the following protocol: 95°C for 2 minutes, and 40 cycles of
162 95°C for 15 seconds and 60°C for 30 seconds, in a MyIQ Real-Time PCR Detection
163 System (BioRad). After the amplification phase, a dissociation curve was obtained to
164 ensure that there was only one product amplified. All reactions were run in triplicate
165 and for, at least, 3 biological replicates. Statistical analysis of relative expression results
166 was carried out with the REST software tool (Pfaffl et al., 2002). RNA expression was
167 calculated in relation to the expression of U6 in experiments intended to measure
168 mRNAs and miRNAs, or to Actin 5c in experiments intended to measure only mRNAs.
169 Primer sequences used are indicated in Supplementary Table S2.

170

171 *2.5. RNAi and treatments with dsRNA in vivo*

172

173 Basic procedures for RNAi experiments were as described by Rubio et al.
174 (2013). Details on the dsRNAs targeting Ago1 (GenBank accession number
175 HF912424), Ago2 (HF912425), Atrophin (HF912426) and PolyH, a sequence from
176 *Autographa californica* nucleopolyhedrovirus, K01149, used as control dsRNA
177 (dsPolyH) are also detailed in Rubio et al. (2013). The dsRNAs were injected at the
178 chosen doses in 1 µL volume in *B. germanica* females freshly emerged to the fifth

179 (penultimate, N5) nymphal stage (N5D0). Effects on the targeted transcript were
180 examined by qRT-PCR in 4-day-old N5 (N5D4) or in freshly emerged sixth (last)
181 nymphal instar (N6D0), depending on the experiment. The primers used to prepare the
182 dsRNAs are indicated in the Supplementary Table S2. To study the effects of an alien
183 dsRNA, freshly emerged N5 were injected with 3 µg of dsPolyH in 1 µL volume of
184 aqueous solution or with 1 µL of water, and Ago1 and Ago2 expression was measured 6
185 hours later.

186

187 2.6. Experiments of RNAi in vitro

188

189 *B. germanica* embryonic cells UM-BGE-1 (Kurtti and Brooks, 1977) were
190 grown in suspension at 25°C in L15 medium (Sigma), modified as recommended by
191 Munderloh and Kurtti (1989). Briefly, the pH was adjusted to 6.5 with sodium
192 hydroxide and the medium was complemented with 5% fetal bovine serum (GIBCO),
193 1% lipoprotein-cholesterol concentrate (Sigma) and 50U/ml penicillin+50 µg/ml
194 streptomycin (GIBCO). The cells were collected by centrifugation, washed twice in
195 PBS and re-suspended in fresh cell culture medium at a density of 10⁶ cells/ml. Two
196 hours after transferring the cells to the plate, the chosen dsRNA (dsPolyH, dsAgo1 or
197 dsAgo2 at a final concentration of 30 nM) was added along with FuGENE Transfection
198 Reagent (Promega), at a proportion 3/1 dsRNA/FuGENE, in medium without serum.
199 Six hours later, complete medium was added to allow cells grow normally. Then,
200 dsAtro was added 24 hours later at the same concentration and conditions. The effect of
201 the treatments on transcript levels was examined 24 hours after the dsAtro treatment.

202

203 3. Results

204

205 3.1. *B. germanica* Ago1 and Ago2 in a phylogenetic context

206

207 Before proceeding with our functional studies, we wanted to confirm that the
208 available Ago1 and Ago2 sequences of *B. germanica* (GenBank HF912424 and
209 HF912425, respectively) were the right orthologues of these proteins in this species. For
210 this purpose, we obtained a representative set of Argonaute 1 and 2 sequences from
211 insects (see the Supplementary Table S1), as well as the sequences of Argonaute 3, Piwi
212 and aubergine from *D. melanogaster* and *B. germanica*, which were used as external

213 groups. A phylogenetic analysis revealed that Ago1 and Ago2 fall into two respective
214 nodes that cluster into the Argonaute subfamily group. On the other hand, Ago3+ Piwi-
215 aubergine cluster in another node, which is the sister group of Ago1+Ago2 (Fig. 1). Our
216 results confirm that *B. germanica* Ago1 and Ago2 robustly cluster into the respective
217 nodes of the Ago1 and Ago2 subfamilies. The analysis also allowed the identification of
218 one Ago3 and two Piwi-aubergine orthologues in *B. germanica*. Moreover, the structure
219 of Ago1, Ago2 and Piwi proteins of *B. germanica* show the canonical organization in
220 domains of each one, homologous to that found in reference species like *D.*
221 *melanogaster* (Supplementary Fig. S1).

222

223 3.2. General effects of Ago1 and Ago2 depletion

224

225 Doses of 3.75 or 1.5 μg of dsAgo1 administered to freshly emerged fifth
226 (penultimate) instar nymphs (N5D0) provoked 100% mortality. Controls (treated with 3
227 μg of dsPolyH) (n=10) molted to normal N6, 6 days after the treatment, and then to
228 normal adults. The dsAgo1-treated insects (n=10) died either during the molting to N6
229 or just after molting (Supplementary Fig. S2). At the highest dose, Ago1 mRNA levels
230 were significantly depleted (38% as average), whereas those of Ago2 were practically
231 unaffected (Fig. 2A). Subsequently, we used a dose of 0.5 μg of dsAgo1 administered to
232 freshly emerged N5. In this experiment, Ago1 mRNA levels were also reduced (33% as
233 average, although the differences with respect to the controls were not statistically
234 significant), whereas Ago2 mRNA levels were practically unaffected (Fig. 2A). In this
235 experiment, controls (n=40) again molted normally to N6 and then to adults.
236 Conversely, the treatment with 0.5 μg of dsAgo1 in N5 (n=80) gave the following
237 phenotypes: 54 treated insects (68 %) died in the process of molting from N5 to N6; 13
238 insects (16%) molted to an apparently normal N6, remained in this stage for 40-50 days,
239 and then died; 5 insects (6%) molted to normal N6 6 days after the treatment, and then
240 molted again to an intermediate nymph-adult 8 days later; and 8 insects (10%) molted to
241 malformed adults 8 days after treatment (Fig. 2B and Supplementary Fig. S2). The
242 intermediate nymph-adult phenotype had a blackish coloration and a general nymphal
243 morphology, but the wings were rudimentary and completely wrinkled. The malformed
244 adult phenotype showed the yellowish coloration and general features typical of the
245 adult, but the wings not properly extended and the abdomen was flattened
246 dorsoventrally (Fig. 2B).

247 For Ago2, we carried out equivalent RNAi experiments, using a dose of 2.5 μ g
248 of dsAgo2 administered to freshly emerged N5. Transcript measurements showed that
249 Ago2 mRNA levels were significantly depleted (86% as average), whereas those of
250 Ago1 showed average values similar to controls, although with high deviations, which
251 suggest that Ago1 might have been targeted by dsAgo2 in some cases (Fig. 2C). Both
252 groups, Ago2-depleted (n=10) and control (n=10), molted to normal N6, and then to
253 normal adults. The only difference was the length of the N6 stage, which was 25%
254 longer in Ago2-depleted (Fig. 2D).

255

256 3.3. Effects on the miRNA pathway

257

258 First, we studied the influence of Ago1 on miRNA levels, using the following
259 mature miRNAs as case studies: bantam (bantam-3-p), let-7 (let-7-5p), miR-1 (miR-1-
260 3p), miR-10 (miR-10-5p), miR-34 (miR-34-5p), miR-184 (miR-184-3p) and miR-276
261 (miR-276-3p). Moreover, we also studied the “passenger” strand of two of them: miR-
262 10* (miR-10-3p) and miR-276* (miR-276-5p). We treated freshly emerged N5 with 0.5
263 μ g of dsAgo1, and we measured the levels of these miRNAs in freshly emerged N6
264 (N6D0). Bantam, let-7, miR-1, miR-184, and miR-276 were significantly down-
265 regulated, miR-10 tended to be down-regulated, miR-34 was practically unaffected,
266 whereas miR-10* and miR-276* were significantly up-regulated (Fig. 3A).

267 Using an equivalent approach, we studied the effect of Ago2-depletion. Freshly
268 emerged N5 were treated with 2.5 μ g of dsAgo2, and the miRNAs were measured in
269 freshly emerged N6. Results showed that only let-7 and miR-1 were significantly down-
270 regulated, whereas all the others were not significantly affected, although miR-10*,
271 miR-184 and miR-276 tended to be down-regulated (Fig. 3B).

272

273 3.4. Effects on the siRNA pathway

274

275 Next, we studied the influence of Ago1 and Ago2 on the siRNA pathway. Our
276 approach consisted of assessing whether Ago1 or Ago2 depletion impaired the RNAi
277 efficiency when targeting a given transcript. As a case-study transcript we used
278 Atrophin, which is efficiently depleted by RNAi in *B. germanica* (Rubio et al., 2013). In
279 a first set of experiments we treated freshly emerged N5 with either dsAgo1 (0.5 μ g) or
280 dsAgo2 (2.5 μ g), and, subsequently, with dsAtro (3 μ g) just after the molt to N6.

281 Controls were treated in a similar way with dsPolyH (3 μ g in N5 and 3 μ g in N6). All
282 control insects (n=20) molted to normal N6 and then to normal adults. The treatment
283 with dsPolyH in N5 and dsAtro in N6 (n=20) triggered a significant decrease of
284 Atrophin mRNA levels (55% as average) (Fig. 4A). The insects molted from N6 to
285 adults with partially extended and wrinkled wings (Fig. 4B), as a consequence of slower
286 and imperfect ecdysis. As expected, these effects are coincident with those reported by
287 Rubio et al. (2013).

288 All insects treated with dsAgo1 in N5 and dsAtro in N6 (n=15) died the day after
289 the second treatment. Those treated with dsAgo2 in N5 and dsAtro in N6 (n=20) molted
290 from N6 to normal adults or had, at most, the forewings (tegmina) slightly separated
291 from one another (Fig. 4B). On day 4 of N6 the levels of Ago2 mRNA were still
292 significantly lower (50% as average) than in the controls, whereas Atrophin levels were
293 similar to the controls (Fig. 4A).

294 The lethal effects of Ago1 depletion in these in vivo experiments prevented us
295 demonstrating whether Ago1 operates in the siRNA pathway and the RNAi process. For
296 this reason, we decided to follow an approach in vitro using the *B. germanica*
297 embryonic cells UM-BGE-1. The cells were first treated with dsPolyH, dsAgo1, or
298 dsAgo2, and then 24 hours later with dsPolyH or dsAtro. Thereafter, 24 hours after the
299 last treatment, the levels of the corresponding mRNAs were measured. The results
300 showed that Ago1 depletion practically did not affect the RNAi effects of dsAtro.
301 Conversely, depletion of Ago2 precluded RNAi effects, as shown by the high levels of
302 Atrophin mRNA in these experiments, despite the treatment with dsAtro (Fig. 4C).

303

304 3.5. Effects of an alien dsRNA on Ago1 and Ago2 expression

305 Finally, we wondered whether a dsRNA treatment would stimulate the
306 expression of Ago2, as occurs with Dicer-2, as reported by Lozano et al. (2012). Freshly
307 emerged N5 were injected with 3 μ g of dsPolyH in 1 μ L volume of aqueous solution or
308 with 1 μ L of water, and expression was measured 6 hours later. Results showed that
309 Ago2 was significantly up-regulated (34% as average) by the dsPolyH treatment,
310 whereas Ago1 was unaffected. As a positive control, we measured the expression of
311 Dicer-2, which was also up-regulated (127% as average) (Fig. 4D), as expected
312 according to Lozano et al. (2012).

313

314 4. Discussion and conclusions

315

316 4.1. *AGO and Piwi family genes in B. germanica*

317

318 Sequence comparisons and analyses led to the unequivocal identification of the
319 orthologues of Ago1 and Ago2 in *B. germanica*. The topology obtained in our
320 phylogenetic tree is similar to that found by Wang et al. (2013). Thus, Ago1 and Ago2
321 belong to the Ago subfamily, while Ago3 and Piwi-aubergine pertain to the Piwi
322 subfamily (Aravin et al., 2007). The shorter branches of the Ago1 node with respect to
323 those of Ago2 indicate that Ago1 sequences are much more conserved than those of
324 Ago2. This is perhaps related to the high evolvability of the Ago2 gene, which is
325 frequently duplicated and has a highly variable copy number in arthropods (Palmer and
326 Jiggins, 2015). Our study led to the characterization of the orthologues of Ago3 and
327 Piwi-aubergine. The topology of this node suggests that there were independent
328 duplications of Piwi-like genes in the respective *D. melanogaster* and *B. germanica*
329 branches, precluding the establishment of direct Piwi and aubergine orthologues
330 between the two species. For this reason, we named the two *B. germanica* sequences
331 Piwi-1 and Piwi-2. Finally, our discovery of an Ago3 orthologue in the cockroach *B.*
332 *germanica* contradicts the hypothesis that this gene was lost in Dictyoptera (Dowling et
333 al., 2016). The organization of the respective protein families also shows the close
334 similarity between the Ago1 and Ago2 families, and the divergence of the Piwi family.

335

336 4.2. *Ago1 is a vital gene in B. germanica*

337 Depletion of Ago1 in N5 using 3.75 or 1.5 μ g doses of dsRNA provoked 100%
338 mortality, suggesting that Ago1 is involved in vital processes in *B. germanica*, at least
339 in late nymphal instars. The 0.5 μ g dose still provoked 68% mortality, whereas the
340 survivors that molted to N6 showed three different phenotypes: a permanent N6 stage, a
341 subsequent molt to an intermediate nymph-adult, and a subsequent molt to a malformed
342 adult. These results indicate that Ago1 is crucial in molting and metamorphosis. In the
343 beetle *Tribolium castaneum*, RNAi depletion of Ago1 in larvae produced developmental
344 defects and impaired pupation (Tomoyasu et al., 2008). Further studies showed that
345 Ago1 depletion up-regulated the expression of Methoprene-tolerant (Met) and Krüppel
346 homolog-1 (Kr-h1), crucial transducers of the antimetamorphic signal of juvenile
347 hormone (Belles and Santos, 2014; Jindra et al., 2015), as well as resulting in defects in
348 ecdysis and the pupa, and concomitant mortality in late larval or pupal stages, effects

349 that are mediated by miRNAs (Wu et al., 2017). In *B. germanica*, the phenotypes
350 observed are reminiscent of those obtained when depleting Dicer-1, which consequently
351 affects miRNA levels and impairs adult morphogenesis (Gomez-Orte and Belles, 2009).
352 Other work revealed that miR-2, which targets Kr-h1, is predominantly responsible for
353 the phenotype observed (Belles, 2017; Lozano et al., 2015). Therefore, we presume that
354 the severe phenotypes observed after depleting Ago1 derive from miRNA deficiencies
355 (see next section). Conversely, the efficient depletion of Ago2 in N5 using a 2.5 µg dose
356 of dsRNA produced no phenotypic effects but merely resulted in a slight delay of the
357 imaginal molt. This suggests that Ago2 is not needed for housekeeping homeostasis in
358 *B. germanica* nymphs.

359

360 4.3. *B. germanica* preferentially use Ago1 in the miRNA pathway, but can also use Ago2

361

362 To test the participation of Ago1 and Ago2 in the production of miRNAs, we
363 analyzed the change in expression of different miRNAs after depleting Ago1 or Ago2.
364 The levels of most of the miRNAs measured in Ago1-depleted specimens were down-
365 regulated or had a tendency to down-regulation, with the exception of miR-10* and
366 miR-276*, which were significantly up-regulated. This suggests that in *B. germanica*
367 miRNAs generally follow the canonical miRNA pathway, through which the duplex
368 miR/miR* is sorted by Ago1 that then selects the mature strand (Czech et al., 2009).
369 Nevertheless, this is not always the case. The sorting of miR/miR* duplexes between
370 Ago1 and Ago2 depends on the duplex structure and sequence information. In *D.*
371 *melanogaster*, mismatches at central positions direct duplex loading towards Ago1,
372 whereas central pairing increases Ago2 loading. In addition, Ago1-loaded miRNAs
373 have a very strong preference for U at 5', whereas Ago2-loaded miRNAs show a
374 moderate preference for C (Czech et al., 2009; Ghildiyal et al., 2010). Furthermore, and
375 particularly in the case of miR/miR* duplexes with high complementarity, the strand
376 with the thermodynamically less stable 5' end is more often retained (Czech et al.,
377 2009; Okamura et al., 2009). These peculiarities produce that, whereas most of the
378 small RNAs that come from miR/miR* duplexes are mature miRNAs loaded into Ago1,
379 Ago2 was significantly depleted of mature miRNAs and enriched for miRNAs* (Czech
380 et al., 2009; Ghildiyal et al., 2010). This may explain the up-regulation of miR-10* and
381 miR-276* in our Ago1-depleted specimens. In control animals, mature miR-10 and
382 miR-276 levels are much higher than their corresponding miR-10* and miR-276* (Ylla

383 et al., 2017). However, our present results indicate that Ago1 depletion reduces the
384 mature and increases the star strands of these miRNAs, pointing to a loading of the
385 duplexes into the Ago2 complex and an increase in miR-10* and miR-276* selection.
386 Consistent with these notions, Ago1 depletion in *D. melanogaster* S2 cells triggers a
387 reduction of mature miR-276a and an increase of miR-276a* (Czech et al., 2009),
388 suggesting that miR-276a* is preferentially loaded into the Ago2 complex (Okamura et
389 al., 2009). Finally, as Ago2 depletion triggers a decrease of miR-1 and let-7 levels, we
390 propose that these two miRNAs are preferentially selected by the Ago2 complex. As
391 indicated above, Ago1 depletion also produces a decrease in miR-1 and let-7 levels,
392 pointing to Ago1 sorting for these duplexes, this being the more common pathway for
393 most miRNAs (Czech and Hannon, 2011). However, the duplexes miR-1/miR1* and
394 let-7/let-7* show high complementarity in the middle of the structure (Ylla et al., 2017),
395 which could alternatively direct them, to some extent, to Ago2. miR-10* also tends to
396 be reduced in Ago2-depleted specimens, suggesting that some of the processing of miR-
397 10/miR-10* is carried out by Ago2. On the other hand, miR-276* levels do not change
398 with this treatment, indicating that Ago2 is not the main pathway for processing miR-
399 276/miR-276*.

400

401 4.4. Ago2 operates in the siRNA pathway in *B. germanica*

402

403 Our experiments combining treatments with dsAgo1, dsAgo2 and dsAtro, in
404 vivo and in vitro, indicated that in *B. germanica* Ago2 is required for the RNAi
405 mechanism, whereas Ago1 is dispensable. These results suggest that in *B. germanica*
406 RNAi mechanisms and siRNA sorting depend on Ago2, whereas Ago1 does not appear
407 to play relevant roles in this process. This is quite general in insects, as first
408 demonstrated in *D. melanogaster* (Czech et al., 2009; Förstemann et al., 2007) and then
409 in other species, like the hemipteran *Nilaparvata lugens* (Xu et al., 2013), the
410 lepidopteran *Bombyx mori* (Li et al., 2015) and the coleopteran *Diabrotica virgifera*
411 (Vélez et al., 2016). However, a few studies report that Ago1 is involved in the RNAi
412 process. For example, Williams and Rubin (2002) described that mutations in the Ago1
413 gene in *D. melanogaster* suppress RNAi in embryos. However, the effect results from a
414 reduced ability to degrade mRNA in response to dsRNA in vitro, suggesting that Ago1
415 functions downstream of siRNA production. More recently, Yoon et al. (2016) reported
416 that depletion of Ago1 and aubergine/Piwi in the Colorado potato beetle *Leptinotarsa*

417 *decemlineata*, reduces the RNAi effect against IAP (Inhibitor of apoptosis). Moreover,
418 dsAgo1 reduced siRNAs formation from the GFP dsRNA, suggesting that Ago1 plays a
419 role in the production of siRNAs. The authors propose that the action of Ago1 is at the
420 level of intracellular transport of dsRNA and/or recruitment of Dicer enzymes, thus,
421 upstream of siRNA production (Yoon et al., 2016).

422

423 4.5. Alien dsRNA stimulates the expression of Ago2 but not Ago1

424

425 Interestingly, an injection of dsPolyH stimulated the expression of Ago2, in
426 comparison with an injection of water, which parallels the results obtained in a previous
427 work reporting that Dicer-2 is also stimulated by dsPolyH (Lozano et al., 2012).
428 Conversely, dsPolyH did not affect the expression of Ago1. In RNA-based antiviral
429 immunity in insects, dsRNAs are recognized as molecules associated with pathogens
430 and, as a defensive mechanism, they are processed into siRNAs by host Dicer-2 (Ding,
431 2010). Moreover, evidence for a role of Dicer-2 as a sensor of viral infection and as a
432 key antiviral defense element beyond the RNAi pathway has been demonstrated in *D.*
433 *melanogaster*, where Dicer-2 mediates the induction of the antiviral gene Vago
434 (Deddouche et al., 2008). Indeed, sensing alien RNAs could have been a specialized
435 function of Dicer-2 after the duplication of the ancestral Dicer gene (Lozano et al.,
436 2012). The parallel stimulation of Ago2 by an alien dsRNA suggests that it could also
437 play a sensor role associated to Dicer-2, and again supports that Ago2 specializes in the
438 siRNA sorting, whereas Ago1 does not seem to participate in that pathway.

439

440 4.6. Conclusions

441

442 In *D. melanogaster*, Ago1 associates with miRNAs, and Ago2 with siRNAs
443 (Czech et al., 2009). However, there are exceptions to the rule, and inverse relationships
444 have been described, Ago2 sorting miRNAs and Ago1 influencing the RNAi process,
445 although probably upstream or downstream of siRNA sorting. This study focused on the
446 parallel Argonaute sorting of small RNAs, and our results show that *B. germanica*
447 preferentially uses Ago1 in the miRNA pathway, but can also use Ago2. Conversely,
448 Ago2 would operate in the RNAi, in siRNA sorting, whereas Ago1 does not appear to
449 be relevant in this process. These basic associations are equivalent to those observed in

450 *D. melanogaster*, implying that they have been evolutionary conserved from at least
451 cockroach to flies, and possibly stem from the last common ancestor of extant insects.

452

453 **Transparency document**

454 The Transparency document associated with this article can be found, in online
455 version.

456

457 **Acknowledgements**

458 This work was supported by the Spanish Ministry of Economy and
459 Competitiveness (grants CGL2012–36251 and CGL2015–64727-P to X.B., and
460 CGL2016–76011-R to M.D.P. and J.L.M.) and the Catalan Government (2017 SGR
461 1030). It also received financial assistance from the European Fund for Economic and
462 Regional Development (FEDER funds to X.B., M.D.P. and J.L.M.). Thanks are also
463 due to Raul Montañez and Jesús Lozano, for helpful discussions, and to Timothy Kurtti
464 (University of Minnesota, USA) for providing the UM-BGE-1 cell line.

465

466

467 **References**

468

- 469 **Aravin, A. A., Hannon, G. J. and Brennecke, J.** (2007). The Piwi-piRNA pathway
470 provides an adaptive defense in the transposon arms race. *Science* **318**, 761–764.
- 471 **Bartel, D. P.** (2009). MicroRNAs: target recognition and regulatory functions. *Cell* **136**,
472 215–233.
- 473 **Belles, X.** (2010). Beyond *Drosophila*: RNAi in vivo and functional genomics in
474 insects. *Annu. Rev. Entomol.* **55**, 111–128.
- 475 **Belles, X.** (2017). MicroRNAs and the Evolution of Insect Metamorphosis. *Annu. Rev.*
476 *Entomol.* **62**, 111–125.
- 477 **Belles, X. and Santos, C. G.** (2014). The MEKRE93 (Methoprene tolerant-Krüppel
478 homolog 1-E93) pathway in the regulation of insect metamorphosis, and the
479 homology of the pupal stage. *Insect Biochem. Mol. Biol.* **52**, 60–68.
- 480 **Belles, X., Cristino, A. S., Tanaka, E. D., Rubio, M. and Piulachs, M. D.** (2012).
481 Insect microRNAs: from molecular mechanisms to biological roles. In *Insect*
482 *Molecular Biology and Biochemistry* (ed. L. I. Gilbert), pp. 30–56. Amsterdam:
483 Elsevier-Academic Press.

484 **Bernstein, E., Caudy, A. A., Hammond, S. M. and Hannon, G. J.** (2001). Role for a
485 bidentate ribonuclease in the initiation step of RNA interference. *Nature* **409**, 363–
486 366.

487 **Carthew, R. W. and Sontheimer, E. J.** (2009). Origins and Mechanisms of miRNAs
488 and siRNAs. *Cell* **136**, 642–55.

489 **Czech, B. and Hannon, G. J.** (2011). Small RNA sorting: matchmaking for
490 Argonautes. *Nat. Rev. Genet.* **12**, 19–31.

491 **Czech, B., Zhou, R., Erlich, Y., Brennecke, J., Binari, R., Villalta, C., Gordon, A.,
492 Perrimon, N. and Hannon, G. J.** (2009). Hierarchical rules for Argonaute loading
493 in *Drosophila*. *Mol. Cell* **36**, 445–456.

494 **Deddouche, S., Matt, N., Budd, A., Mueller, S., Kemp, C., Galiana-Arnoux, D.,
495 Dostert, C., Antoniewski, C., Hoffmann, J. A. and Imler, J.-L.** (2008). The
496 DExD/H-box helicase Dicer-2 mediates the induction of antiviral activity in
497 *drosophila*. *Nat. Immunol.* **9**, 1425–1432.

498 **Ding, S.-W.** (2010). RNA-based antiviral immunity. *Nat. Rev. Immunol.* **10**, 632–644.

499 **Dowling, D., Pauli, T., Donath, A., Meusemann, K., Podsiadlowski, L., Petersen,
500 M., Peters, R. S., Mayer, C., Liu, S., Zhou, X., et al.** (2016). Phylogenetic origin
501 and diversification of RNAi pathway genes in insects. *Genome Biol. Evol.* **8**,
502 3784–3793.

503 **Förstemann, K., Horwich, M. D., Wee, L., Tomari, Y. and Zamore, P. D.** (2007).
504 *Drosophila* microRNAs are sorted into functionally distinct argonaute complexes
505 after production by dicer-1. *Cell* **130**, 287–297.

506 **Ghildiyal, M., Xu, J., Seitz, H., Weng, Z. and Zamore, P. D.** (2010). Sorting of
507 *Drosophila* small silencing RNAs partitions microRNA* strands into the RNA
508 interference pathway. *RNA* **16**, 43–56.

509 **Gomez-Orte, E. and Belles, X.** (2009). MicroRNA-dependent metamorphosis in
510 hemimetabolan insects. *Proc. Natl. Acad. Sci. U. S. A.* **106**, 21678–21682.

511 **Grimaldi, D. and Engel, M. S.** (2005). *Evolution of the insects*. Cambridge University
512 Press.

513 **Hartig, J. V., Tomari, Y. and Förstemann, K.** (2007). piRNAs-the ancient hunters of
514 genome invaders. *Genes Dev.* **21**, 1707–1713.

515 **Jindra, M., Belles, X. and Shinoda, T.** (2015). Molecular basis of juvenile hormone
516 signaling. *Curr. Opin. Insect Sci.* **11**, 39–46.

517 **Kuhn, C.-D. and Joshua-Tor, L.** (2013). Eukaryotic Argonautes come into focus.

518 *Trends Biochem. Sci.* **38**, 263–271.

519 **Kurtti, T. J. and Brooks, M. A.** (1977). Isolation of cell lines from embryos of the
520 cockroach, *Blattella germanica*. *In Vitro* **13**, 11–7.

521 **Larkin, M. A., Blackshields, G., Brown, N. P., Chenna, R., McGettigan, P. A.,**
522 **McWilliam, H., Valentin, F., Wallace, I. M., Wilm, A., Lopez, R., et al.** (2007).
523 Clustal W and Clustal X version 2.0. *Bioinformatics* **23**, 2947–2948.

524 **Lee, Y. S., Nakahara, K., Pham, J. W., Kim, K., He, Z., Sontheimer, E. J. and**
525 **Carthew, R. W.** (2004). Distinct roles for Drosophila Dicer-1 and Dicer-2 in the
526 siRNA/miRNA silencing pathways. *Cell* **117**, 69–81.

527 **Lewis, S. H., Salmela, H. and Obbard, D. J.** (2016). Duplication and diversification of
528 dipteran Argonaute genes, and the evolutionary divergence of Piwi and aubergine.
529 *Genome Biol. Evol.* **8**, 507–18.

530 **Li, Z., Zeng, B., Ling, L., Xu, J., You, L., Aslam, A. F. M., Tan, A. and Huang, Y.**
531 (2015). Enhancement of larval RNAi efficiency by over-expressing Argonaute2 in
532 *Bombyx mori*. *Int. J. Biol. Sci.* **11**, 176–85.

533 **Lozano, J., Gomez-Orte, E., Lee, H.-J. and Belles, X.** (2012). Super-induction of
534 Dicer-2 expression by alien double-stranded RNAs: an evolutionary ancient
535 response to viral infection? *Dev. Genes Evol.* **222**, 229–235.

536 **Lozano, J., Montañez, R. and Belles, X.** (2015). MiR-2 family regulates insect
537 metamorphosis by controlling the juvenile hormone signaling pathway. *Proc. Natl.*
538 *Acad. Sci. U. S. A.* **112**, 3740–3745.

539 **Martinez, J., Patkaniowska, A., Urlaub, H., Lührmann, R. and Tuschl, T.** (2002).
540 Single-stranded antisense siRNAs guide target RNA cleavage in RNAi. *Cell* **110**,
541 563–574.

542 **Meister, G.** (2013). Argonaute proteins: functional insights and emerging roles. *Nat.*
543 *Rev. Genet.* **14**, 447–459.

544 **Munderloh, U. G. and Kurtti, T. J.** (1989). Formulation of medium for tick cell
545 culture. *Exp. Appl. Acarol.* **7**, 219–229.

546 **Okamura, K., Liu, N. and Lai, E. C.** (2009). Distinct mechanisms for microRNA
547 strand selection by Drosophila Argonautes. *Mol. Cell* **36**, 431–444.

548 **Palmer, W. J. and Jiggins, F. M.** (2015). Comparative genomics reveals the origins
549 and diversity of arthropod immune systems. *Mol. Biol. Evol.* **32**, 2111–2129.

550 **Pfaffl, M. W., Horgan, G. W. and Dempfle, L.** (2002). Relative expression software
551 tool (REST) for group-wise comparison and statistical analysis of relative

552 expression results in real-time PCR. *Nucleic Acids Res.* **30**, e36.

553 **Poelchau, M., Childers, C., Moore, G., Tsavatapalli, V., Evans, J., Lee, C.-Y., Lin,**
554 **H., Lin, J.-W. and Hackett, K.** (2015). The i5k Workspace@NAL--enabling
555 genomic data access, visualization and curation of arthropod genomes. *Nucleic*
556 *Acids Res.* **43**, D714–719.

557 **Rubio, M., Montañez, R., Perez, L., Milan, M. and Belles, X.** (2013). Regulation of
558 atrophin by both strands of the mir-8 precursor. *Insect Biochem. Mol. Biol.* **43**,
559 1009–1014.

560 **Shabalina, S. A. and Koonin, E. V** (2008). Origins and evolution of eukaryotic RNA
561 interference. *Trends Ecol. Evol.* **23**, 578–587.

562 **Siomi, H. and Siomi, M. C.** (2009). On the road to reading the RNA-interference code.
563 *Nature* **457**, 396–404.

564 **Siomi, M. C., Sato, K., Pezic, D. and Aravin, A. A.** (2011). PIWI-interacting small
565 RNAs: the vanguard of genome defence. *Nat. Rev. Mol. Cell Biol.* **12**, 246–258.

566 **Stamatakis, A.** (2014). RAxML version 8: a tool for phylogenetic analysis and post-
567 analysis of large phylogenies. *Bioinformatics* **30**, 1312–1313.

568 **Swarts, D. C., Makarova, K., Wang, Y., Nakanishi, K., Ketting, R. F., Koonin, E.**
569 **V, Patel, D. J. and van der Oost, J.** (2014). The evolutionary journey of
570 Argonaute proteins. *Nat. Struct. Mol. Biol.* **21**, 743–753.

571 **Tomoyasu, Y., Miller, S. C., Tomita, S., Schoppmeier, M., Grossmann, D. and**
572 **Bucher, G.** (2008). Exploring systemic RNA interference in insects: a genome-
573 wide survey for RNAi genes in *Tribolium*. *Genome Biol.* **9**, R10.

574 **Vélez, A. M., Khajuria, C., Wang, H., Narva, K. E. and Siegfried, B. D.** (2016).
575 Knockdown of RNA interference pathway genes in Western Corn Rootworms
576 (*Diabrotica virgifera virgifera* Le Conte) demonstrates a possible mechanism of
577 resistance to lethal dsRNA. *PLoS One* **11**, e0157520.

578 **Wang, G.-H., Jiang, L., Zhu, L., Cheng, T.-C., Niu, W.-H., Yan, Y.-F. and Xia, Q.-**
579 **Y.** (2013). Characterization of Argonaute family members in the silkworm,
580 *Bombyx mori*. *Insect Sci.* **20**, 78–91.

581 **Williams, R. W. and Rubin, G. M.** (2002). Argonaute1 is required for efficient RNA
582 interference in *Drosophila* embryos. *Proc. Natl. Acad. Sci. U. S. A.* **99**, 6889–6894.

583 **Wu, W., Xiong, W., Li, C., Zhai, M., Li, Y., Ma, F. and Li, B.** (2017). MicroRNA-
584 dependent regulation of metamorphosis and identification of microRNAs in the red
585 flour beetle, *Tribolium castaneum*. *Genomics* **109**, 362–373.

586 **Xu, H.-J., Chen, T., Ma, X.-F., Xue, J., Pan, P.-L., Zhang, X.-C., Cheng, J.-A. and**
587 **Zhang, C.-X.** (2013). Genome-wide screening for components of small interfering
588 RNA (siRNA) and micro-RNA (miRNA) pathways in the brown planthopper,
589 *Nilaparvata lugens* (Hemiptera: Delphacidae). *Insect Mol. Biol.* **22**, 635–647.
590 **Ylla, G., Fromm, B., Piulachs, M.-D. and Belles, X.** (2016). The microRNA toolkit of
591 insects. *Sci. Rep.* **6**, 37736.
592 **Ylla, G., Piulachs, M.-D. and Belles, X.** (2017). Comparative analysis of miRNA
593 expression during the development of insects of different metamorphosis modes
594 and germ-band types. *BMC Genomics* **18**, 774.
595 **Yoon, J.-S., Shukla, J. N., Gong, Z. J., Mogilicherla, K. and Palli, S. R.** (2016).
596 RNA interference in the Colorado potato beetle, *Leptinotarsa decemlineata*:
597 Identification of key contributors. *Insect Biochem. Mol. Biol.* **78**, 78–88.
598

600 **FIGURE LEGENDS**

601

602 Figure 1. Phylogenetic analysis of Ago1 and Ago2 in insects, using Ago3, Piwi and
603 aubergine sequences of *Drosophila melanogaster* and *B. germanica* as external group.
604 The species and accession numbers are indicated in the supplementary Table S1. The
605 protein sequences were aligned using ClustalX and phylogenetic reconstruction with
606 RAxML, based on the maximum-likelihood principle, a JTT matrix, a gamma model of
607 heterogeneity rate, and using empirical base frequencies and estimating proportions.
608 Bootstrap values >50 are indicated at the corresponding node. Scale bar indicates the
609 number of substitutions per site.

610

611

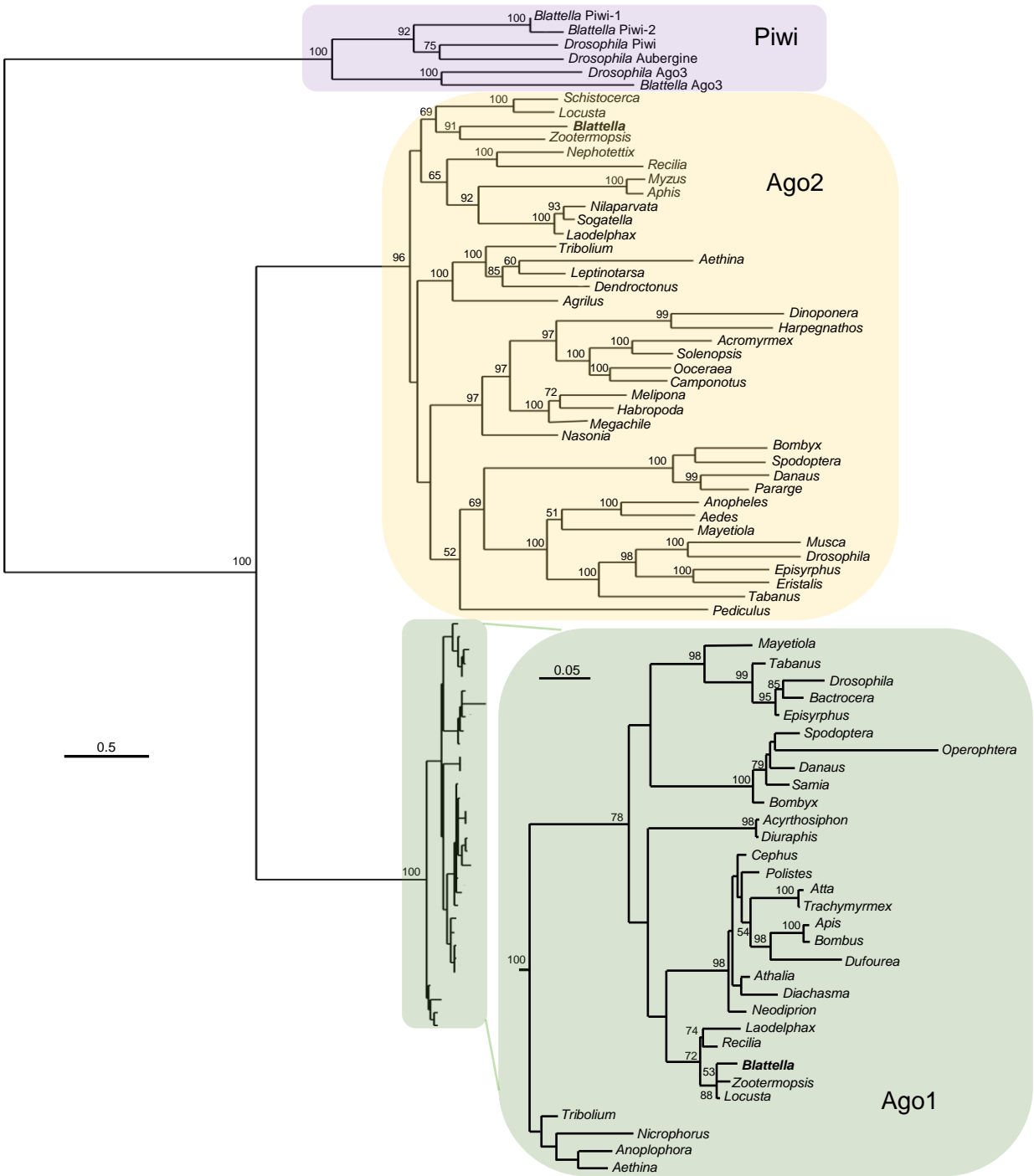
612 Figure 2. Effect of RNAi of Ago1 and Ago2 in *Blattella germanica*. (A) Effects of
613 dsAgo1 treatment at the doses indicated on Ago1 and Ago2 transcript levels. (B)
614 Representative phenotypes resulting from the treatment with dsAgo2 at a dose of 0.5
615 μg . (C) Effects of dsAgo2 treatment at a dose of 2.5 μg on Ago1 and Ago2 transcript
616 levels. (D) Effects of dsAgo2 treatment at a dose of 2.5 μg on the length of the last
617 nymphal instar (N6). dsAgo1 or dsAgo2 was administered on female nymphs freshly
618 ecdysed to the penultimate instar (N5D0) and transcript levels were measured 4 days
619 later (N5D4). In A and C, each point represents at least three biological replicates and is
620 normalized against the controls (reference value corresponding to dsPolyH treatment,
621 which is 5.35 ± 2.63 for Ago1 and 18.22 ± 7.57 for Ago2, copies per 1000 copies of U6,
622 $n=3$ in both cases); the asterisk indicates statistically significant differences with respect
623 to controls ($p < 0.05$) according to the REST software tool (Pfaffl et al., 2002). In D,
624 each point represents 10 biological replicates and the asterisk indicates statistically
625 significant differences with respect to controls ($p < 0.05$) according to the student's *t*-
626 test.

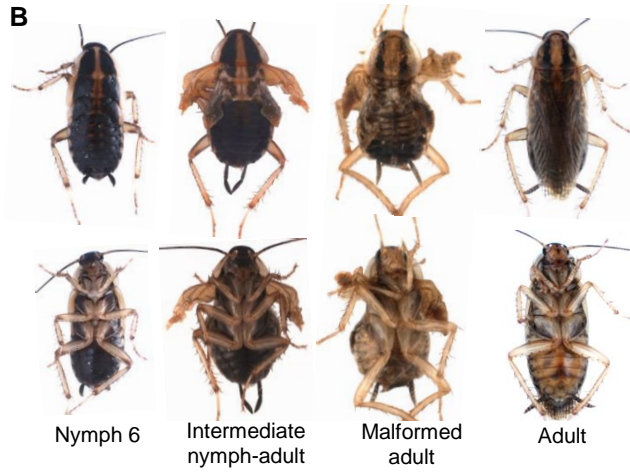
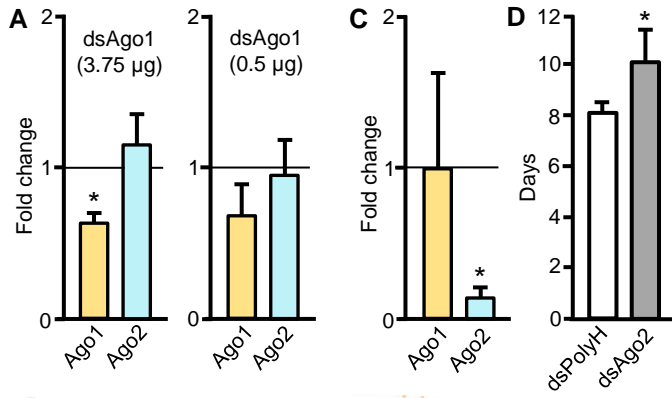
627

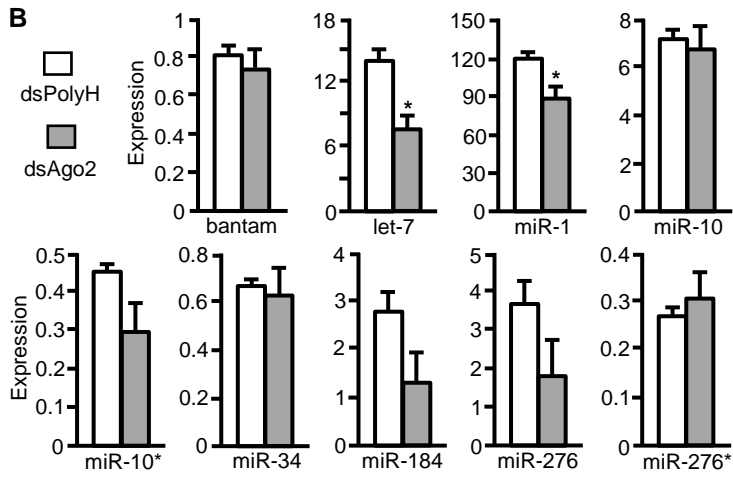
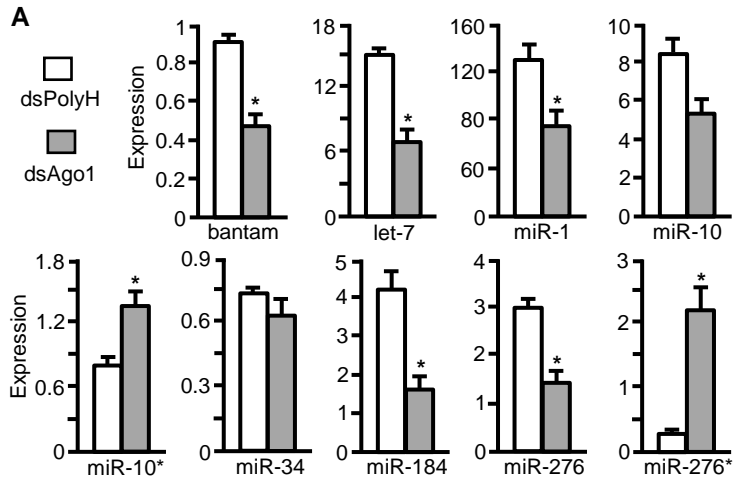
628

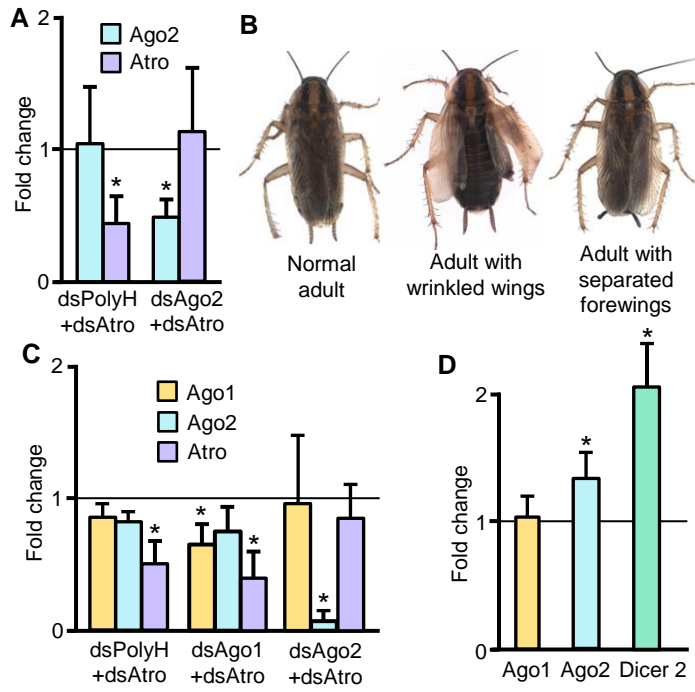
629 Figure 3. Effect of Ago1 or Ago2 depletion on the expression of miRNAs in *Blattella*
630 *germanica*. dsAgo1 (0.5 μg) or dsAgo2 (2.5 μg) were administered on in freshly
631 ecdysed fifth instar female nymphs (N5D0), and miRNAs were measured just after
632 molting to the next instar(N6D0). Data are expressed as miRNA copies per 10 copies of
633 U6. Each point represents three biological replicates; the asterisk indicates statistically

634 significant differences with respect to controls ($p < 0.05$) according to the REST
635 software tool (Pfaffl et al., 2002).
636
637 Figure 4. Effect of Ago1 or Ago2 depletion on RNAi of Atrophin in *Blattella*
638 *germanica*, and effect of dsPolyH on Ago1 and Ago2 expression. (A) Effects in vivo of
639 a first treatment of dsPolyH (3 μ g) and a second treatment of dsAtro (3 μ g), or a first
640 treatment of dsAgo2 (2.5 μ g) and a second treatment of dsAtro (3 μ g) on Atrophin
641 (Atro) and Ago2 mRNA levels; the first treatment was performed in freshly emerged
642 female nymphs in fifth instar (N5) and the second just after the molt to the next instar
643 (N6). (B) Phenotypes resulting from the treatment described in panel “a”. (C) Effects in
644 UM-BGE-1 cells cultured in vitro of a first treatment with dsPolyH, dsAgo1 or dsAgo2,
645 and a second treatment with dsAtro; the second treatment was performed 24 hours after
646 the first one, and mRNAs were measured 24 hours after the second treatment; dsRNAs
647 were used at a final concentration of 30 nM. (D) Effect of dsPolyH treatment on Ago1
648 Ago2 and Dicer-2 expression; dsPolyH was administered to female nymphs freshly
649 ecdysed to the penultimate instar (N5D0) and transcript levels were measured 6 hours
650 later. Data on transcript levels are expressed as mRNA copies per 1000 copies of U6 (A
651 and C) or Actin 5c (D); each point represent three biological replicates and is
652 normalized against the controls (reference value corresponding to dsPolyH treatment,
653 which in A is 66.26 ± 18.97 for Ago2 and 11.58 ± 5.38 for Atro, copies per 1000 copies
654 of U6, $n=3$ in both cases; in C is 14.35 ± 4.31 for Ago1, 129.67 ± 8.34 for Ago2 and
655 46.31 ± 7.10 for Atro, copies per 1000 copies of U6, $n=3$ in all cases; and in D is 7.28
656 ± 1.20 for Ago1, 26.50 ± 3.27 for Ago2 and 7.07 ± 0.65 for Dicer-2, copies per 1000
657 copies of Actin 5c, $n=3$ in all cases); the asterisk indicates statistically significant
658 differences with respect to controls ($p < 0.05$) according to the REST software tool
659 (Pfaffl et al., 2002).









Conserved association of Argonaute 1 and 2 proteins with miRNA and siRNA pathways throughout insect evolution, from cockroaches to flies

Mercedes Rubio, Jose Luis Maestro, Maria-Dolors Piulachs and Xavier Belles

SUPPLEMENTARY FILES

Supplementary Table S1. Name of the species and the protein sequences used in the phylogenetic analysis.

Supplementary Table S2. Primers used to prepare the dsRNA for RNAi experiments, and to measure expression levels by qRT-PCR.

Supplementary Figure S1. Sequence organization of Ago1, Ago2 and Piwi proteins from *Blattella germanica* and *Drosophila melanogaster*.

Supplementary Figure S2. Effect of RNAi of Ago1 in *Blattella germanica* in terms of percentage of the different phenotypes obtained.

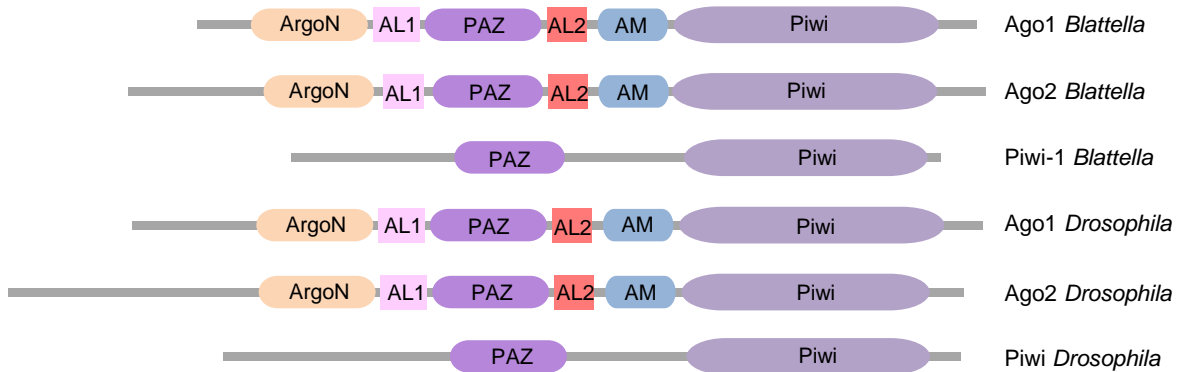
Supplementary Table S1. Name of the species and the protein sequences used in the phylogenetic analysis.

Species	Protein name	Accession number	Description in NCBI
<i>Acromyrmex echinator</i>	Ago2	EGI64275.1	protein argonaute-2
<i>Acyrtosiphon pisum</i>	Ago1	XP_003240620.1	protein argonaute-2
<i>Aedes aegypti</i>	Ago2	ACR56327.1	argonaute 2
<i>Aethina tumida</i>	Ago1	XP_019871683.1	Protein argonaute-2 isoform X1
	Ago2	XP_019874184.1	protein argonaute-2-like
<i>Agrilus planipennis</i>	Ago2	AJF15705.1	argonaute-2
<i>Anopheles darlingi</i>	Ago2	ETN67307.1	argonaute 2
<i>Anoplophora glabripennis</i>	Ago1	XP_018574613.1	protein argonaute-2 isoform X1
<i>Aphis glycines</i>	Ago2	AFZ74933.1	Ago2
<i>Apis mellifera</i>	Ago1	XP_006571833.1	argonaute-2 isoform X2
<i>Athalia rosae</i>	Ago1	XP_012252331.1	argonaute-2 isoform X2
<i>Atta colombica</i>	Ago1	XP_018046590.1	argonaute-2 isoform X2
<i>Bactrocera dorsalis</i>	Ago1	XP_011201159.1	argonaute-2 isoform X2
<i>Blattella germanica</i>	Piwi-1	BGER020794-PA	--
	Piwi-2	Bger_17094	--
	Ago1	CCV01212.1	Argonaute-1
	Ago2	CCV01213.1	Argonaute-2
	Ago3	Bger_01037	--
<i>Bombus terrestris</i>	Ago1	XP_012170889.1	protein argonaute-2
<i>Bombyx mori</i>	Ago1	NP_001095931.1	Argonaute 1
	Ago2	NP_001036995.2	argonaute 2
<i>Camponotus floridanus</i>	Ago2	XP_019882937.1	protein argonaute-2
<i>Cephus cinctus</i>	Ago1	XP_015587083.1	protein argonaute-2
<i>Danaus plexippus</i>	Ago1	OWR47741.1	argonaute 1
	Ago2	OWR52773.1	argonaute 2
<i>Dendroctonus ponderosae</i>	Ago2	XP_019768859.1	protein argonaute-2-like
<i>Diachasma alloeum</i>	Ago1	XP_015114288.1	protein argonaute-2 isoform X2
<i>Dinoponera quadriceps</i>	Ago2	XP_014485297.1	protein argonaute-2-like
<i>Diuraphis noxia</i>	Ago1	XP_015380491.1	protein argonaute-2 isoform X1
<i>Drosophila melanogaster</i>	Piwi	AAD08705.1	Piwi
	Aub	CAA64320.1	Aubergine
	Ago1	NP_001246314.1	Argonaute-1, isoform D
	Ago2	AGB94575.1	argonaute 2, isoform E
	Ago3	AFW19999.1	argonaute 3
<i>Dufourea novaeangliae</i>	Ago1	XP_015433893.1	protein argonaute-2
<i>Episyrphus balteatus</i>	Ago1	ALC79969.1	argonaute 1
	Ago1	ALC79939.1	argonaute 2
<i>Eristalis pertinax</i>	Ago2	ALC79938.1	argonaute 2
<i>Habropoda laboriosa</i>	Ago2	KOC70760.1	Protein argonaute-2
<i>Harpegnathos saltator</i>	Ago2	XP_011150889.1	protein argonaute-2
<i>Laodelphax striatella</i>	Ago1	AIY24302.1	argonaute 1
	Ago2	AIY24303.1	Argonaute 2
<i>Leptinotarsa decemlineata</i>	Ago2	AKQ00044.1	Ago2a protein
<i>Locusta migratoria</i>	Ago1	GO85968.1	argonaute 1
	Ago2	AGO85972.1	argonaute 2
<i>Mayetiola destructor</i>	Ago1	AFX89034.1	argonaute 1
	Ago2	AFX89029.1	argonaute 2b
<i>Megachile rotundata</i>	Ago2	XP_012149383.1	Protein argonaute-2
<i>Melipona quadrifasciata</i>	Ago2	KOX67889.1	Protein argonaute-2
<i>Musca domestica</i>	Ago2	XP_011292642.1	protein argonaute-2 isoform X2
<i>Myzus persicae</i>	Ago2	XP_022175637.1	protein argonaute-2-like

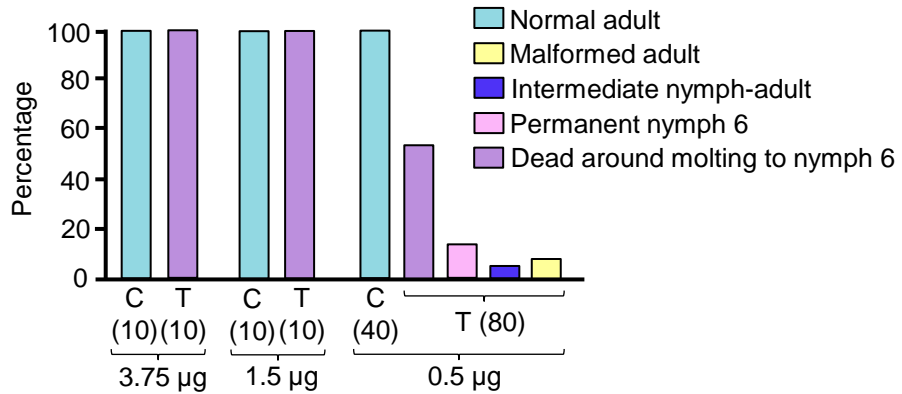
<i>Nasonia vitripennis</i>	Ago2	XP_008214883.1	protein argonaute-2-like
<i>Neodiprion lecontei</i>	Ago1	XP_015523555.1	protein argonaute-2 isoform X1
<i>Nephotettix cincticeps</i>	Ago2	APF46960.1	argonaute-2
<i>Nicrophorus vespilloides</i>	Ago1	XP_017786022.1	Protein argonaute-2 isoform X1
<i>Nilaparvata lugens</i>	Ago2	AGH30327.1	argonaute-2
<i>Ooceraea biroi</i>	Ago2	XP_011351606.1	protein argonaute-2
<i>Operophtera brumata</i>	Ago1	KOB76405.1	Protein argonaute
<i>Pararge aegeria</i>	Ago2	JAA87692.1	Argonaute 2
<i>Pediculus humanus</i>	Ago2	XP_002422648.1	protein argonaute-2, putative
<i>Polistes dominula</i>	Ago1	XP_015171510.1	protein argonaute-2 isoform X1
<i>Recilia dorsalis</i>	Ago1	AMN92166.1	argonaute-1
	Ago2	AMN92165.1	argonaute-2
<i>Samia ricini</i>	Ago1	AID68365.1	argonaute 1
<i>Schistocerca gregaria</i>	Ago2	AFY13246.1	argonaute-2
<i>Sogatella furcifera</i>	Ago2	AGE12620.1	agonaute 2
<i>Solenopsis invicta</i>	Ago2	XP_011157934.1	protein argonaute-2
<i>Spodoptera litura</i>	Ago1	AHC98009.1	argonaute 1
	Ago2	AHC98010.1	argonaute 2
<i>Tabanus bromius</i>	Ago1	ALC79971.1	Argonaute 1
	Ago2	ALC79937.1	argonaute 2
<i>Trachymyrmex zeteki</i>	Ago1	KYQ52776.1	Protein argonaute-2
<i>Tribolium castaneum</i>	Ago1	KYB26000.1	Argonaute 1
	Ago2	NP_001107828.1	Argonaute-2b
<i>Zootermopsis nevadensis</i>	Ago1	XP_021931335.1	protein argonaute-2
	Ago2	XP_021932646.1	protein argonaute-2-like

Supplementary Table S2. Primers used to prepare the dsRNA for RNAi experiments, and to measure expression levels by qRT-PCR. Fw: Forward, Rv: Reverse.

dsRNA/PCR	mRNA/ miRNA	Sequence (5'-3')
dsRNA	Ago1 Fw	CCTCTTCCCATAGGAAATGACA
	Ago1 Rv	TCCATCAGGAGATGAGAAAAA
	Ago2 Fw	AAGGGCTGGCTACAATCAGA
	Ago2 Rv	AGCAGTCTTTGAACCGAGGA
	Atrophin Fw	ACAGGAGTCAGAGTGCTATTTT
	Atrophin Rv	TATGGAGAAGTGATAGTTTCAATA
	PolyH Fw	CCTACGTGTACGACAACAAGTACT
	PolyH Rv	ATGAAGGCTCGACGATCCTAATCA
qRT-PCR	Ago1 Fw	CACTCACTGTGGGACCATGA
	Ago1 Rv	CTCCTCGTCACATTGCACAC
	Ago2 Fw	GCAAGGACCATGCAGAGAAT
	Ago2 Rv	AGACTGATGCGATGCAGTGA
	Atrophin Fw	GGTTACCTCCCCAGTGCATA
	Atrophin Rv	CCAAATGCTCCAATTCCAGT
	bantam-3p	TGAGATCATTGTGAAAGCTGATT
	Dicer-2 Fw	TCGGAATTTGTTGACGGATG
	Dicer-2 Rv	AACATACCCAACGTATCAATGTGG
	Let-7-5p	TGAGGTAGTAGGTTGTATAGT
	miR-1-3p	TGGAATGTAAAGAAGTATGGAG
	miR-10-5p	ACCCTGTAGATCCGAATTTGT
	miR-10-3p*	AAATTCGGTTCTAGAGAGGTTT
	miR-34-5p	TGGCAGTGTGGTTAGCTGGTTG
	miR-184-3p	GACGGAGAAGTATAAGGGC
	miR-276-5p*	AGCGAGGTATAGAGTTCCTACG
	miR-276-3p	TAGGAACTTCATACCGTGCT
	U6	CGATACAGAGAAGATTAGCATGG
	Actin 5c Fw	AGCTTCCTGATGGTCAGGTGA
	Actin 5c Rv	TGTCGGCAATTCCAGGGTACATGGT



Supplementary Figure S1. Sequence organization of Ago1, Ago2 and Piwi proteins from *Blattella germanica* and *Drosophila melanogaster* obtained from Pfam (<https://pfam.xfam.org/>). ArgoN: N-terminal domain of argonaute. AL1: Argonaute linker 1 domain (ArgoL1). PAZ: PAZ domain. AL2: Argonaute linker 2 domain (ArgoL2). AM: Mid domain of argonaute (ArgoMid). Piwi: Piwi domain. Piwi-2, aubergine and Ago3 proteins have the same organization than Piwi/Piwi-1.



Supplementary Figure S2. Effect of RNAi of Ago1 in *Blattella germanica* in terms of percentage of the different phenotypes obtained. C: Control (treated with 3 µg of dsPolyH); T: Treated with dsAgo1. The doses used of dsAgo1 (µg) and the number of replicates in each experiment (in parenthesis) is also indicated.